

Method to Determine Maximum Allowable Sinterable Silver Interconnect Size

A. A. Wereszczak,^{*} M. C. Modugno,^{*} S. B. Waters,^{*} D. J. DeVoto,[§] and P. P. Paret[§]

^{*} Oak Ridge National Laboratory, Oak Ridge, TN 37831

[§] National Renewable Energy Laboratory, Golden, CO 80401

Abstract

The use of sintered-silver for large-area interconnection is attractive for some large-area bonding applications in power electronics such as the bonding of metal-clad, electrically-insulating substrates to heat sinks. Arrays of different pad sizes and pad shapes have been considered for such large area bonding; however, rather than arbitrarily choosing their size, it is desirable to use the largest size possible where the onset of interconnect delamination does not occur. If that is achieved, then sintered-silver's high thermal and electrical conductivities can be fully taken advantage of. Toward achieving this, a simple and inexpensive proof test is described to identify the largest achievable interconnect size with sinterable silver. The method's objective is to purposely initiate failure or delamination. Copper and invar (a ferrous-nickel alloy whose coefficient of thermal expansion (CTE) is similar to that of silicon or silicon carbide) disks were used in this study and sinterable silver was used to bond them. As a consequence of the method's execution, delamination occurred in some samples during cooling from the 250°C sintering temperature to room temperature and bonding temperature and from thermal cycling in others. These occurrences and their interpretations highlight the method's utility, and the herein described results are used to speculate how sintered-silver bonding will work with other material combinations.

Key words: silver, sintering, interconnection, residual stress, coefficient of thermal expansion

Introduction

The use of low-temperature sintered-silver continues to gain traction as evidenced by ever-growing number of internationally-conducted studies devoted to its application [e.g., see Refs. 1-11 for some examples].

In addition to the interconnection between die and substrate, use of sintered-silver for large-area interconnection is also attractive for some large-area bonding applications in power electronics such as the bonding of metal-clad substrates to heat sinks (see Fig. 1). Arrays of different pad sizes and pad shapes have been considered for such large area bonding [10] with the motive to provide an integral and passive strain relief mechanism to always limit the amount of imposed strain. But it is also desirable to use the largest possible size as long as the onset of interconnect delamination does not occur. If that maximization is achieved, then sintered-silver's high thermal and electrical conductivities can be fully taken advantage with that interconnection array pattern.

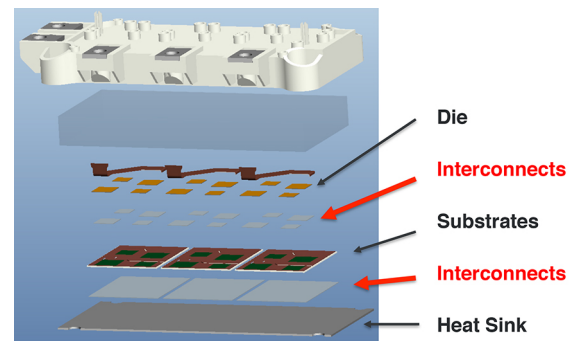


Figure 1. Sintered-silver candidacy for die-to-substrate and substrate-to-heat sink interconnections.

If the sintered-silver interconnection area is too large, then coefficient of thermal expansion (CTE) mismatches among the system's material constituents will cause sufficiently high shear strains to result in the onset of undesirable delamination. An image of such is shown in Fig. 2 [12].

Such delamination is undesirable and the materials pairing of what is shown in Fig 2 indicates that the areal size of its sintered-silver interconnect was too large. It decreases the allowable area for thermal (and electrical) conduction resulting in higher heat (and electrical) fluxes going through the remaining bonded area. Consequently, this can cause an avalanching effect resulting in service temperature further increasing in the device, a greater rate of additional delamination, etc., leading to potential complete debonding of the interconnect and overall loss of intended function.

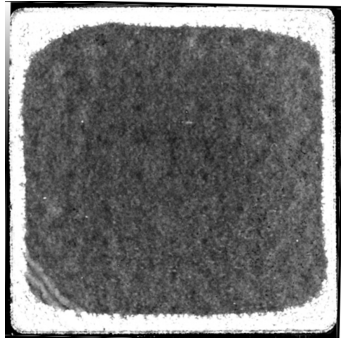


Figure 2. Example of perimeter delamination in a 50 mm x 50 mm (i.e., large) sintered silver interconnection [12].

There are two options to manage delamination. One is to design the interconnect size and shape so delamination never initiates, and the other is to somehow manage or arrest the delamination should it initiate. Further description of these two options is facilitated by the fatigue diagrams shown in Fig. 3, and means and descriptions for generating their curves are described elsewhere [e.g., Ref. 13]. Preventing the onset of delamination is accomplished by ensuring that a threshold stress intensity, K_0 , is never attained in service for the interconnect system. Alternatively, if delamination does initiate in service (i.e., the stress intensity in the interconnect system, K , exceeds K_0), then there is potential to manage it provided K never attains a critical stress intensity, K_c . The ability to manage that is easier if the interconnect system's fatigue resistance is high. Referring to Fig. 3, a higher fatigue resistance is represented by a higher-valued fatigue exponent, n .

Of those two options, designing to prevent delamination initiation is obviously more attractive. If that is accomplished, then the initial interconnect area shall exist in perpetuity to provide sustained and sought-after thermal and electrical transfer.

The likelihood of the onset of delamination decreases with the decrease in pad size (and for pad shapes too that do not have sharp corners). Unfortunately, that smaller size also decreases the area for heat transfer, so a compromise must be struck between having the largest bond size as possible but not so large that delamination will initiate.

Toward preventing the onset of delamination in sintered-silver interconnect systems, a simple and inexpensive proof test is described here to identify the largest achievable interconnect size. The method's objective is to purposely initiate failure or delamination. Copper and invar (a ferrous-nickel alloy whose CTE is similar to that of silicon, Si, or silicon carbide, SiC) disks were used in this study and sinterable silver was used to bond them. As a consequence of the method's execution, delamination occurred in some circumstances from the cool-down to room temperature from the 250°C sintering temperature and from thermal cycling in others. These occurrences and their interpretations highlight the method's utility and their discussion follows.

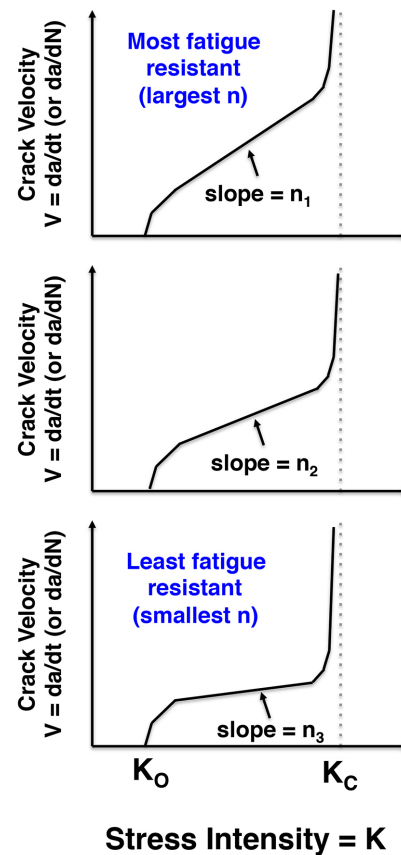


Figure 3. Classical fatigue representations as a function of fatigue exponent (n).

Processing and Testing

Copper and invar disks, with a 25-mm diameter and 2-mm thickness, were fabricated and silver plated. Aluminum, although not considered in this study, logically could have been considered (e.g., paired with copper or with invar). Examples of the disks prior to, and after, plating are shown in Fig. 4, and cross-sectional microstructures and dimensions of the platings are shown in Fig. 5.

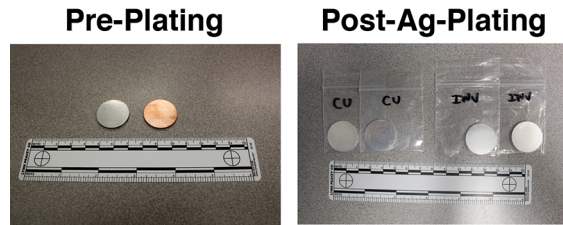


Figure 4. Invar and copper disks (left) prior to plating and (right) after their silver plating. The disks have a diameter of 25 mm.

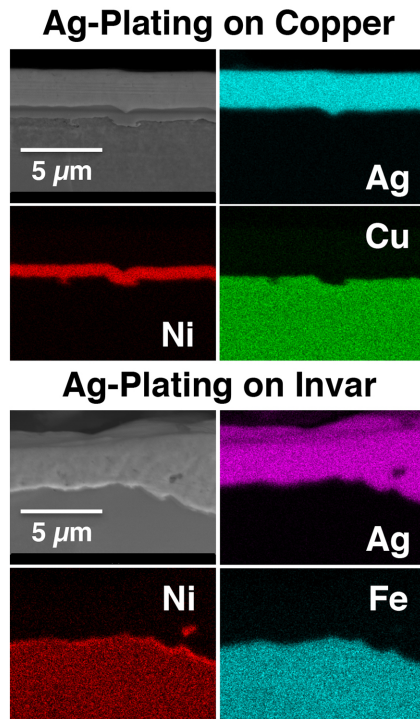


Figure 5. Microstructure, thicknesses, and chemistries of the used platings on the copper and invar disks. Images generated with scanning electron microscopy and companion energy dispersive spectroscopy.

The plated disks were used in three different combinations of couples that are illustrated in Fig. 6. Each of those three couples were bonded with sinterable silver with a pad diameter of 10, 18, or 22 mm.

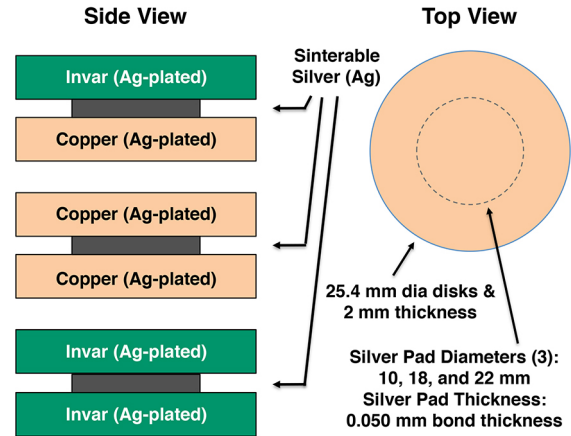


Figure 6. Schematic showing how CTE-induced residual stress was purposely varied through choice of disk materials and bonding size.

Loctite Ablestik SSP 2020 (Henkel) silver paste was stencil printed using a HMI Presco 485 printer. A circular print pad shape was chosen to avoid creating localized regions of high stress intensity intrinsically caused by corners (e.g., such that results when using squares). The print pattern was concentrically deposited onto one of the plated disks and dried at 100°C in nitrogen for 2 hours. The companion top plated disk was then mounted and the disk couple was sintered at 250°C for 1 hour at a pressure of 1 MPa. Specimens were cooled while under stress. A strain-free temperature of 250°C was used for supportive finite element analysis.

All the post-processed disks were mechanically proof-tested by uniaxially applying 1 MPa of shear stress at room temperature. All passed this mechanical proof-test despite scanning acoustic microscopy imaging indicating that delamination had indeed occurred in some of the bonded couples.

Acoustic microscopy imaging was co-utilized with thermal cycling to track any changes in delamination caused by the CTE-mismatch-induced residual stresses. The employed thermal cycling waveform was trapezoid and consisted of 5°C/min heating and cooling rates, and dwell periods at 170°C for 5 minutes and -40°C for 15 minutes (relevant temperature extremes for automotive service). All the disks were imaged prior to thermal cyclic

commencement (i.e., 0 cycles), and then imaged every 100 cycles thereafter.

Unfortunately, those samples that had failed from the thermal cycling (conducted at NREL) were lost during shipment back to ORNL by the shipping carrier, so complete failure analysis was impossible.

Results and Discussion

Post-Processing and Pre-Thermal-Cycling

Delamination occurred simply from the cool-down to room temperature from the 250°C bonding process for the copper-invar couple when they were bonded with 18- and 22-mm diameter sintered-silver pads. Delamination did not occur at this stage for this couple when 10-mm diameter sintered-silver pads bonded the copper and invar. The acoustic microscopy images of the as-processed couples are shown in Figs. 7-9 for copper-copper, invar-invar, and copper-invar, respectively.

The sustained shapes of the sintered-silver bonding are evident in Figs. 7-9 and those that had undergone delamination between sintering and subsequent cool-down to room temperature had a Rorschach-like pattern to them.

The areas of those remaining bonding shapes were analyzed by fitting maximum-sized circles completely within their shape. Examples of such are shown in Fig. 10. The radius of such a circle is then dictated by the narrowest lineal dimension of that Rorschach-like pattern, and is therefore a conservative interpretation of the area of that complex shape.

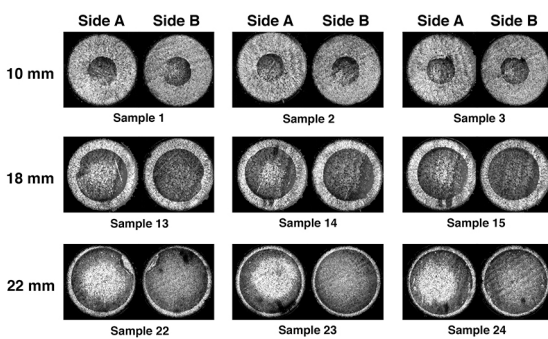


Figure 7. Acoustic microscopy images of the as-processed copper-copper couples bonded with silver. Each of the nine pairings are images captured through opposite directions.

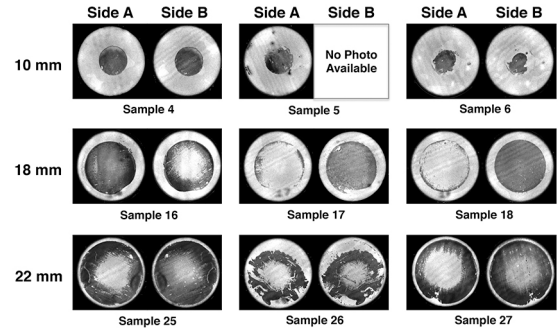


Figure 8. Acoustic microscopy images of the as-processed invar-invar couples bonded with silver. Each of the nine pairings are images captured through opposite directions.

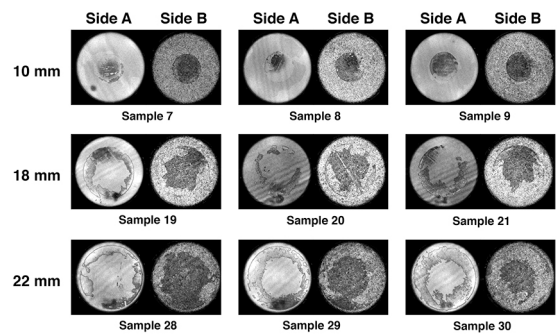


Figure 9. Acoustic microscopy images of the as-processed copper-invar couples bonded with silver. Each of the nine pairings are images captured through opposite directions.

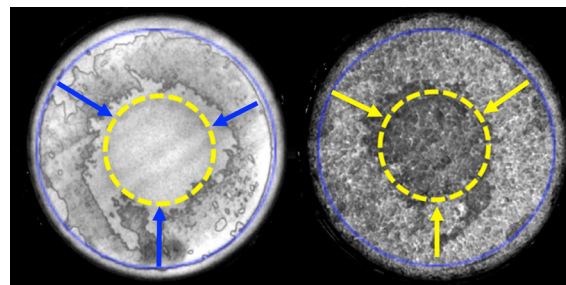


Figure 10. Example of superimposed (dashed) circles on a copper-invar couple used in the analysis of the sustained sintered-silver bond shape. The arrows show the radial ingress from the original printed diameter in this example.

The estimated bond diameters from this analysis are shown in Fig. 11. The printed sintered-silver pad size for all three diameters were maintained in the copper-copper couples, were maintained for the 10- and 18-mm pad diameters for the invar-invar couples, and were only maintained for the 10-mm pad diameter for the copper-invar couple. The copper-invar couples were most affected by their imposed residual stress states.

A large differential in the CTE mismatch relative to the sintered-silver caused delamination for larger bonded areas (i.e., invar-invar couples); however, an asymmetric CTE across (or perpendicular to the plane of) it was more apt to promote the onset of delamination. Such across-the-interconnect CTE asymmetry superimposes in-plane and out-of-plane shear stress resulting in an overall higher (equivalent) stress that is more likely to reach the interconnect system's shear strength and cause the onset of delamination.

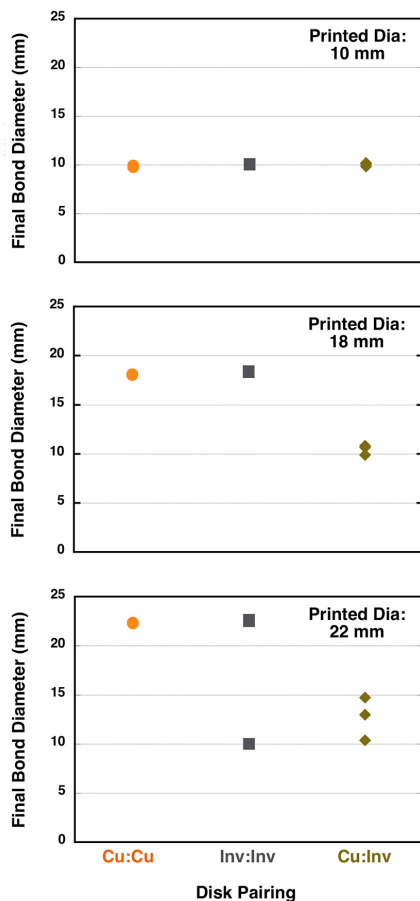


Figure 11. Residual diameter of the sustained bonding of the as-processed couples.

Thermal Cycling

Thermal cycling caused mortality of all the copper-invar couples in less than 400 cycles. This is illustrated in Fig. 12. This observation suggests that subjecting such an interconnect system to this relatively low number of thermal cycles could serve as an effective proof test and eliminate the weakest samples in a population.

There is a high likelihood that failure of the copper-invar couples shown in Fig. 12 occurred at, or about, the -40°C dwell segment of the employed thermal waveform. A comparison of the estimated residual stresses in the sintered-silver pad at room temperature and at -40°C is featured in Fig. 13. The magnitude of the equivalent stresses is the highest at the coldest temperature of the waveform (i.e., at the greatest ΔT from the processing or assumed strain free temperature of 250°C) so it is reasonable to consider that each couple's respective catastrophic failure initiated at that thermal waveform segment.

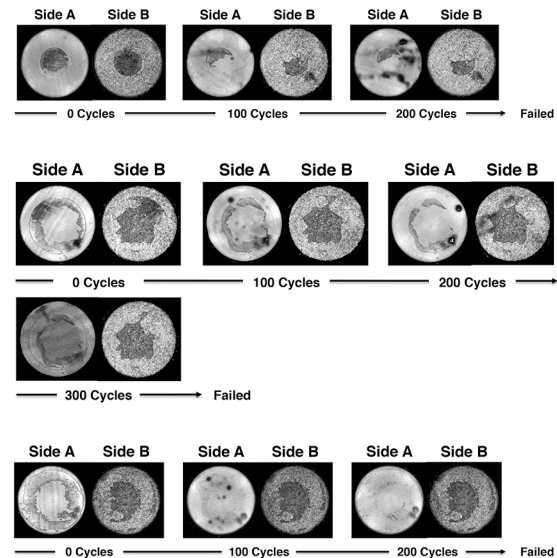


Figure 12. Tracked acoustic microscopy images of (top) 10-mm diameter, and (middle) 18-mm diameter, and (bottom) 22-mm diameter bonded copper-invar couples. All failed in less than 400 thermal cycles.

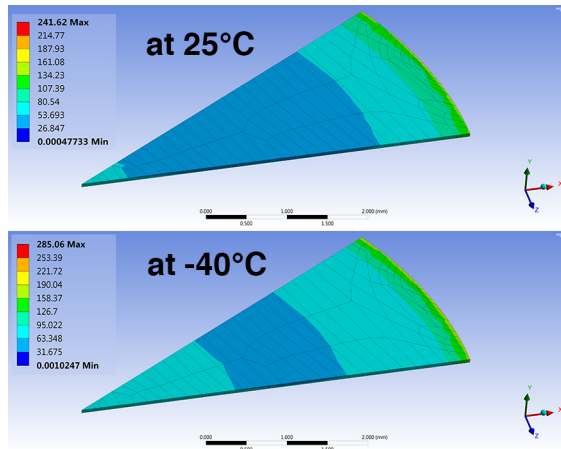


Figure 13. Residual (von Mises) stress state in the 10-mm-bonded copper-invar couple at room temperature and -40°C . The maximum stress is approximately 20% higher at -40°C than at 25°C .

Such thermal cycling did not cause failure (i.e., fatigue run-out) for copper-copper or invar-invar couples bonded by sintered-silver (up to 22-mm diameter print pads) despite the (in-plane, yet out-of-plane-symmetrical) residual stresses that existed in their sintered-silver interconnects. This response is illustrated by the unchanging images shown in Fig. 14. This further illustrates the deleterious influence of an asymmetric CTE mismatch across the sintered-silver interconnect, and which is schematically illustrated in Fig. 15.

Interpretation of the tracking of the delamination of the thermal-cycling-induced failures suggests that the sintered-silver process used here produced a relatively fatigue-resistant interconnect. That statement is based on there not being identifiable continuous delamination occurring up to failure of the interconnect system (i.e., catastrophic delamination must have initiated and entirely occurred in less than 100 cycles); this is an indicator of a relatively high fatigue exponent.

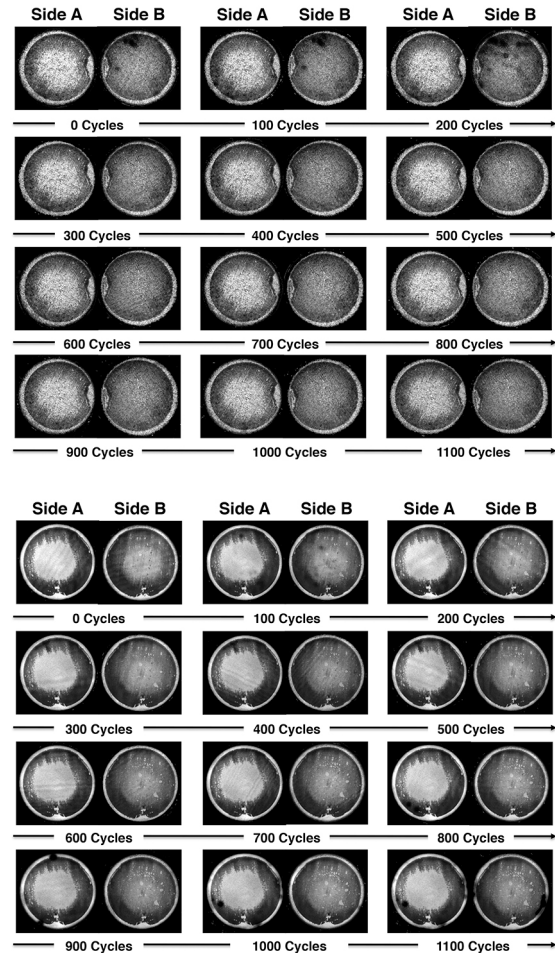


Figure 14. Tracked acoustic microscopy images of the 22-mm-diameter bonded (top) copper-copper and (bottom) invar-invar couples. No delamination initiated through 1100 cycles.

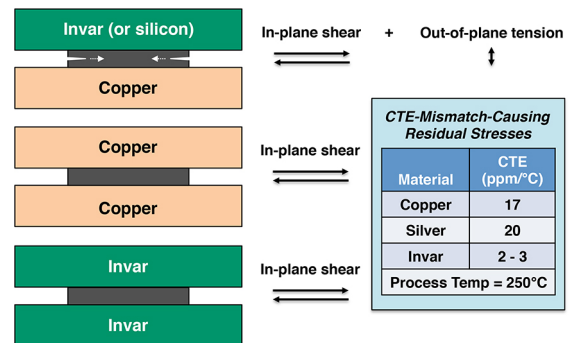


Figure 15. The superpositioning out-of-plane residual stress causes the observed delamination in the copper-invar couples.

A simple and inexpensive approach was described here to identify the largest achievable interconnect size with sinterable silver that will not delaminate. That size is an outcome of all the cumulative effects of numerous independent parameters that each affect that achievable size; those independent parameters are many as illustrated by Fig. 16 [11]. The failure location favored the interface where the top plated disk was mounted on the pre-dried printed silver (prior to sintering). While that was an overall adhesive failure, the exact location of the failure (among the multi-laminated plating and interface with the sintered silver) could not be identified because the failed test specimens were lost in shipping.

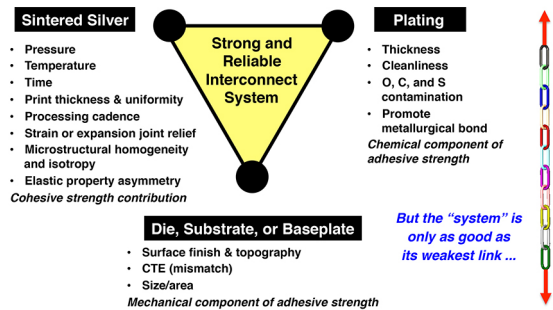


Figure 16. Ultimately the maximum allowable bonding area is a function of many parameters in addition to the CTE mismatches of the bonded materials.

In summation, this method showed that a sintered-silver interconnect having a diameter of at least 22 mm can bond copper to copper or a diameter of at least 10 mm can bond invar to invar. A 10 mm diameter of sintered-silver will fail in thermal cycling if it bonds copper to invar.

Consideration of Other Material Combinations

Speculation of the sintered-silver-bonding quality for other material pairings can be made based on the CTEs of the materials examined in this study (i.e., copper and invar) and the herein-described method. Invar was chosen in the present study because of its CTE-equivalency with those CTEs of silicon and silicon carbide, so the consideration of sintered-silver bondability with silicon (Si) or silicon carbide (SiC) can occur. Copper (Cu) was chosen in the present study; however, aluminum (Al) or molybdenum (Mo) could have alternatively been considered as well. DBC substrates (e.g., with an

aluminum oxide dielectric, or DBC/ Al_2O_3) obviously an important constituent in power electronic modules, so based on the CTEs listed in Table 1, it is reasonable to speculate on the size of sintered-silver bondability between them and other alloys as well.

The anticipated size limitations of sintered-silver bonding of various couples are listed in Table 2. It is reasonable to speculate that the maximum allowable bonding area for sinterable silver decreases with increase in CTE mismatch of the materials the silver is joining.

Table 1. Material CTEs pertaining to Table 2.

Material	Nominal Coefficient of Thermal Expansion ($\times 10^{-6}/^\circ\text{C}$)
Silver	20
Copper	17
Invar	2-3
Silicon	3
Silicon Carbide	4
Aluminum	22
DBC Substrate (with Al_2O_3 dielectric)	8
Molybdenum	5

Table 2. Maximum sizes of sinterable-silver bonding pad diameter as a function of material (or CTE) pairing.

Material Couple	Diameter
Cu - Cu	> 22 mm
Invar - Invar	> 10 mm
Cu - Invar	< 10 mm
Speculation Based on CTEs in Table 1	
<i>In-plane Residual Stress Only:</i>	
Al - Al	> 18 mm
DBC/ Al_2O_3 substrate - DBC/ Al_2O_3 substrate	> 10 mm
Mo - Mo	> 10 mm
<i>In-plane + Out-of-Plane Residual Stress:</i>	
Si - DBC	> 10 mm
SiC - DBC	> 10 mm
DBC/ Al_2O_3 - Cu	< 18 mm
DBC/ Al_2O_3 - Al	< 18 mm
DBC/ Al_2O_3 - Mo	> 10 mm
Cu - Al	> 10 mm
Cu - Mo	< 18 mm
Al - Mo	< 18 mm

Summary

A simple and inexpensive approach was described to identify the largest achievable interconnect size with sinterable silver. That size is an outcome of all the cumulative effects of numerous independent parameters that each affects that achievable size. The method can be viewed as a proof test.

To identify the largest bonding size, the method's objective is to purposely initiate failure or delamination. The method involves making geometrically simple test coupons whose materials have CTEs that match or mimic those of materials used in power electronic devices, and that are bonded by an interconnect material whose bond size is likely to exceed that used in that device.

Copper and invar disks were used and sinterable silver was used to bond them. Aluminum, although not considered in this study, alternatively could have been a matrix material (e.g., paired with copper or with invar) to represent its use as a heat exchanger heat sink. Molybdenum could also have been considered owing to its established use in silicon-controlled rectifiers (SCRs).

Delamination occurred simply from the cool-down to room temperature from the 250°C bonding process for the copper-invar couple when they were bonded with 18- and 22-mm diameter sintered-silver pads. Delamination did not occur in this stage for this couple when 10-mm diameter sintered-silver pads bonded the copper and invar.

A large differential in the CTE mismatch relative to the sintered-silver would cause delamination for larger bonded areas (i.e., the silver-bonded invar-invar couples); however, an asymmetric CTE across (or perpendicular to the interconnect plane of) the sintered-silver interconnect is more apt to promote the onset of delamination. Such across-the-interconnect CTE asymmetry superimposes in-plane and out-of-plane shear stress resulting in an overall higher (equivalent) stress that is more likely to reach the interconnect system's shear strength and cause the onset of delamination.

Thermal cycling (entire coupon at an isothermal temperature for any given temperature of that cycling) caused mortality of all the copper-invar couples by 400 cycles. This suggests that subjecting such an interconnect system to a relatively low number of thermal cycles could serve as an effective proof test. Such thermal cycling did not cause failure for copper-copper or invar-invar couples bonded by sintered-silver (up to 22-mm diameter print pads); this further illustrates the deleterious influence of an asymmetric CTE mismatch across the sintered-silver interconnect.

Interpretation of the tracking of the delamination of the thermal-cycling-induced failures suggests that the sintered-silver process used here produced a relatively fatigue-resistant interconnect. That statement is based on there not being identifiable continuous delamination occurring up to failure of the interconnect system (i.e., catastrophic delamination must have initiated and entirely occurred in less than 100 cycles); this is an indicator of a relatively high fatigue exponent.

Finally, a sintered-silver interconnect having a diameter of at least 22 mm can bond copper to copper or at least 10 mm can bond invar to invar. A 10 mm diameter of sintered-silver will fail in thermal cycling if it bonds copper to invar. Speculation of the sintered-silver-bondability for other material pairings (e.g., silicon, aluminum, molybdenum, and DBC substrates) were made based on each of their respective CTEs.

Acknowledgments

Research co-sponsored by the Propulsion Materials Program and the Electric Drive Technologies Programs, DOE Vehicle Technologies Office, under contract DE-AC05-00OR22725 with UT-Battelle, LLC.

The authors thank USDOE's J. Gibbs and S. Rogers, ORNL's A. Haynes, B. Ozpineci, R. Wiles, and ORNL's A. Haynes, G. -J. Su, Z. Wang for reviewing the manuscript.

References

- [1] S. Klaka and R. Sittig, "Reduction of Thermomechanical Stress by Applying a Low Temperature Joining Technique," pp. 259-264 in *Proc. 6th Int. Symp. Power Semiconductor Devices & ICs*, Davos, Switzerland, (1994).
- [2] Z. Zhang and G. -Q. Lu, "Pressure-Assisted Low-Temperature Sintering of Silver Paste as an Alternative Die-Attach Solution to Solder Reflow," *IEEE Trans. Elect. Pack. Manuf.*, 25:279-283 (2002).
- [3] R. Eisele, J. Rudzki, and M. Kock, "Pressure Sintering for Thermal Stack Assembly," PCIM Europe, Nuremberg, Germany (2007).
- [4] C. Göbl and J. Faltenbacher, "Low Temperature Sinter Technology Die Attachment for Power Electronic Applications," Paper 10.1, CIPS 2010, Nuremberg, Germany.
- [5] E. Schulze, C. Mertens, and A. Lindemann, "Pure Low Temperature Joining Technique Power Module for Automotive Production Needs," Paper 10.2, CIPS 2010, Nuremberg, Germany.
- [6] M. Knoerr and A. Schletz, "Power Semiconductor Joining through Sintering of Silver Nanoparticles: Evaluation of Influence of Parameters Time, Temperature and Pressure on Density, Strength and Reliability," Paper 10.3, CIPS 2010, Nuremberg, Germany.
- [7] T. Licht, R. Speckels, and M. Thoben, "Sintering Technology Used for Interconnection of Large Areas:

- Potential and Limitation for Power Modules," Paper 10.4, CIPS 2010, Nuremberg, Germany.
- [8] W. Schmitt, "Novel Silver Contact Paste Lead Free Solution for Die Attach," Paper 10.5, CIPS 2010, Nuremberg, Germany.
- [9] T. G. Lei, J. N. Calata, G. -Q. Lu, X. Chen, and S. Luo, "Low-Temperature Sintering of Nanoscale Silver Paste for Attaching Large-Area ($> 100 \text{ mm}^2$) Chips," IEEE Trans. Comp. Pack. Tech, 33:98-104 (2010).
- [10] A. A. Wereszczak, D. J. Vuono, Z. Liang, and E. E. Fox, "Sintered Silver Joint Strength Dependence on Substrate Topography and Attachment Pad Geometry," Paper 12.4, 7th International Conference on Integrated Power Electronics Systems (CIPS), Nuremberg, Germany, March 6-8, 2012.
- [11] A. A. Wereszczak, Z. Liang, M. K. Ferber, and L. D. Marlino, "Uniqueness and Challenges of Sintered Silver as a Bonded Interface Material," Journal of Microelectronics and Electronic Packaging, 11:158-165 (2014).
- [12] D. DeVoto, P. Paret, S. Narumanchi, M. Mihalec, "Reliability of Bonded Interfaces for Automotive Power Electronics," Paper IPACK2013-73143, Proceedings of the ASME 2013 International Technical Conference and Exhibitions on Packing and Integration of Electronic and Photonic Microsystems, InterPACK2013, Burlingame, CA, July 16-18, 2013.
- [13] K. Breder and A. A. Wereszczak, Fatigue and Slow Crack Growth, Chapter 6 in *Mechanical Testing and Methodology for Ceramic Design and Reliability*, Eds. D. C. Cranmer and D. W. Richerson, Marcel Dekker, Inc., New York, 1998.